JOURNAL OF MAGNETIC RESONANCE, Series B 106, 101–109 (1995)

Dynamic Nuclear Polarization with Nitroxides Dissolved in Biological Fluids

DANIEL GRUCKER, THIERRY GUIBERTEAU, BERNARD ECLANCHER, JACQUES CHAMBRON, ROBERT CHIARELLI,* ANDRÉ RASSAT,* GUY SUBRA,† AND BERNARD GALLEZ‡

Institut de Physique Biologique, URA 1173 du CNRS, Faculté de Médecine, 4 Rue Kirschléger, 67085 Strasbourg Cedex, France

Received June 17, 1993; revised May 16, 1994

The most widely used free radicals for dynamic nuclear polarization (DNP) experiments or related Overhauser imaging are nitroxides. The DNP parameters in biological fluids were measured in order to provide guidelines for the design of new nitroxides, adapted to the biological applications of DNP. Eighteen nitroxides were studied at a concentration of 1 m*M*. Extrapolation at complete electron paramagnetic resonance saturation and proton longitudinal-relaxation-time measurements enable calculation of the coupling factor between nitroxide free electrons and water protons. In deoxygenated phosphate-buffered solutions, the NMR signal enhancement by DNP ranged from −36.3 to −6.7, and the coupling factor ranged from 0.31 to 0.03. Nitroxides with a long side chain yield poor enhancement, although their relaxivity is far greater than that of nitroxides with small chains. In a 1 m*M* albumin solution, the loss in enhancement factor is mainly caused by the fact that proton relaxation occurs via interactions, not only with the dissolved free radicals but also with the albumin macromolecules. In serum, the enhancement factor is lower than that in an albumin solution, because of the higher protein concentration in serum. In red-blood-cell suspensions, the enhancement factor was further decreased. Two effects contribute to this decrease: first, the increased viscosity due to the presence of red blood cells, and second, the susceptibility effects of the paramagnetism of deoxyhemoglobin. The high sensitivity to oxygen of DNP in phosphate-buffered solution is also greatly reduced when nitroxides are dissolved in blood. In red-blood-cell solutions there is competition between the removal of O_2, which favors proton relaxation by the free radical, and the increase of deoxyhemoglobin, which provides the water protons with another sink of relaxation. On the basis of this study, the properties of nitroxides for use in biological application must fulfill four criteria; i.e., they must have an EPR linewidth narrower than 100 mG, a relaxivity greater than 2.5 $(\text{m}M\,\text{s})^{-1}$, a good stability with a half-life time in biological fluids exceeding 1 hour, and low toxicity.

* Laboratoire de Chimie, URA 1110 du CNRS, Ecole Normale Supérieure, 24 Rue Lhomond, 75231 Paris Cedex 05, France.

† URA 1111 du CNRS, Faculté de Pharmacie, 15 Avenue Charles Flahaut, 34060 Montpellier Cedex, France.

‡ Unité de Chimie Pharmaceutique et de Pharmacognosie, Avenue Emmanuel Mounier 7340, 1200 Bruxelles, Belgique.

INTRODUCTION

Dynamic nuclear polarization (DNP) is a well-known double-magnetic-resonance technique, in which a nuclear magnetic resonance is observed during simultaneous irradiation of an electron paramagnetic resonance. Recently it has been suggested that DNP imaging methods may be used to detect exogenous and endogenous free radicals and to measure the oxygen content of tissues (*1–5*). The most widely used free radicals in DNP experiments in aqueous media are nitroxides. They are stable free radicals, with one unpaired electron in the N–oxyl chemical bond. Although nitroxides are currently used for spin-labeling techniques in order to quantify molecular motion in biological systems by EPR spectroscopy (*6–8*) and for magnetometry at very low magnetic field (*9–11*), to the best of our knowledge, no study of their DNP properties in biological fluids was ever carried out. Studying DNP with nitroxides dissolved in blood is important, not only as a preliminary to pharmacological studies but also because blood is the first body tissue which the nitroxides come into contact with when injected intravenously for DNP imaging or DNP oximetry.

The aim of this work is to measure the DNP parameters which govern the water-proton signal enhancement in biological fluids, in order to provide guidelines for the design of new nitroxides, suited to the biological applications of DNP.

THEORETICAL BACKGROUND

For the convenience of the reader, some theoretical DNP results have been gathered from several sources (*12–14*) and presented here as a brief reminder. These, however, have been restricted to facts relevant to DNP with nitroxides dissolved in water, where the NMR signal enhancement is based on the coupling of the free electrons (spins S) of nitroxides with the protons (spins I) of water molecules. Such a system has, at first approximation, a four-energy-level diagram where the population of the energetic states depends on the relaxation processes which couple the variation of the population

1064-1866/95 $6.00

of the spin states. Figure 1 gives the energy-level diagram with the transition probabilities between these levels. The time-dependent electron–nuclear interactions that generate the relaxation processes of both spins S and I are composed of the dipolar interaction term and the scalar Fermi-contact term. The dipolar interaction term induces relaxation transitions between the spin states, with transition probabilities denoted by w_0^D, w_1^D, and w_2^D (Fig. 1). The scalar term leads to transitions with w_0^{SC} probabilities, and w_{10} corresponds to the reciprocal of the pure solvent spin–lattice relaxation time: $w_{10} = T_{10}^{-1}$.

The theory of Solomon (*15*), which takes into account all the cross-transition probabilities, leads to the basic equation of DNP:

$$\langle I \rangle = \langle I \rangle_0 - \sigma f(\langle S \rangle - \langle S \rangle_0). \qquad [1]$$

$\langle I \rangle$ and $\langle S \rangle$ denote spin polarization, i.e., the difference of the populations of the upper states of proton spins and the electron spins, respectively, minus the population of the lower states divided by the total spin numbers of protons and free electrons, respectively. $\langle I \rangle_0$ and $\langle S \rangle_0$ are the equilibrium polarization of proton spins and free electrons, respectively. The so-called coupling factor σ is defined by

$$\sigma = (w_2^D - w_0^D - w_0^{SC})/(w_2^D + w_0^D + w_0^{SC} + 2w_1^D). \qquad [2]$$

The value of σ can range from -1, assuming pure scalar electron–nuclear interaction, to $+0.5$ in the case of pure dipolar coupling. The so-called leakage factor f, which is defined by

$$f = \frac{w_0^D + w_0^{SC} + 2w_1^D + w_2^D}{w_0^D + w_0^{SC} + 2w_1^D + w_2^D + w_{10}}, \qquad [3]$$

shows how effectively the proton spin is relaxed by the electron spin. It ranges between 0 (no relaxation via the electron–water proton coupling) and 1 (no other relaxation mechanism). The f factor can be written $f = 1 - T_1/T_{10}$, where T_1 is the longitudinal relaxation time of the nitroxide solution and T_{10} is the longitudinal relaxation time of the solvent without nitroxide.

Let K be the nuclear spin of nitrogen; the number of EPR lines of the free radical due to hyperfine interaction is given by $2K + 1$. If one of the nitroxide's EPR lines is saturated, the NMR signal is enhanced or reversed, depending on whether scalar or dipolar coupling dominates the spin–lattice relaxation. The enhancement factor E is given by

$$E = (\langle I \rangle - \langle I \rangle_0)/\langle I \rangle_0 \simeq -\sigma f s |\gamma_S|/\gamma_I, \qquad [4]$$

with

$$s = \frac{\gamma_I}{\gamma_S} \frac{\langle S \rangle - \langle S \rangle_0}{\langle I \rangle_0} \frac{1}{2K+1}.$$

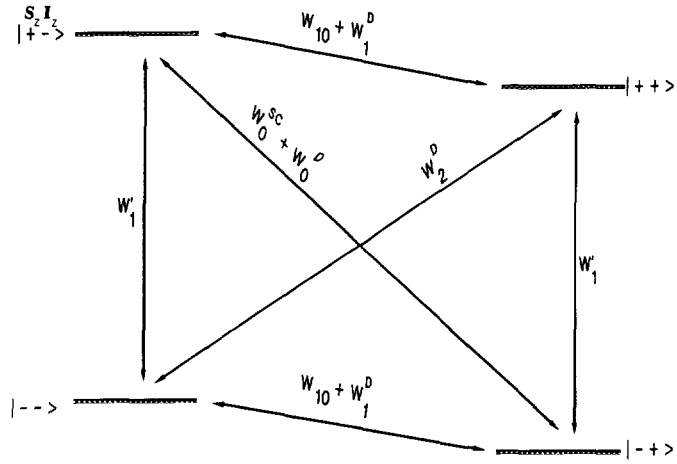

FIG. 1. The energy levels and the transition probabilities of an $S = \frac{1}{2}$, $I = \frac{1}{2}$ coupled system. See text for the definition of the various probabilities.

The magnetogyric ratios of the proton and free electron, respectively, are γ_I and γ_S. At complete saturation of one EPR line, $\langle S \rangle = 0$ and $s = 1/(2K + 1)$. In that case, the proton NMR signal could have a value between $E = -110$, for a pure dipolar coupling, and $E = +220$, for a pure scalar coupling, assuming a leakage factor $f = 1$.

As complete saturation of one of the EPR lines cannot generally be achieved directly, the reciprocal of the measured enhancement factor E is plotted against the reciprocal of the RF power P used to irradiate the EPR line. According to the Bloch equations, the reciprocal of the spin polarization ($\langle S \rangle^{-1}$) is proportional to the reciprocal of the RF power (P^{-1}). Therefore, plotting E^{-1} versus P^{-1} gives a straight line whose intercept is equal to E_∞^{-1}, i.e., the reciprocal enhancement factor at complete EPR saturation:

$$E_\infty = -\tfrac{1}{2}\sigma f |\gamma_S|/\gamma_I. \qquad [5]$$

E_∞ characterizes the overall interaction of free radicals with the solvent. It enables the comparison of the performance of the different nitroxides without being influenced by the factors involved in the saturation of the EPR line such as the EPR linewidth and the instrumental parameters (resonator Q factor and size, RF power, and the duration of EPR irradiation).

If E_∞ is known, measurements of the relaxation times T_1 and T_{10} enable the calculation of the leakage factor f and the coupling factor σ from Eq. [5]. The coupling factor gives information regarding the nature of the interaction between the free electrons and the water protons which is useful for the design of new nitroxides.

MATERIALS AND METHODS

Figure 2 gives the structure, and Table 1 the chemical name and acronyms, of the nitroxides studied. DCH, DCP,

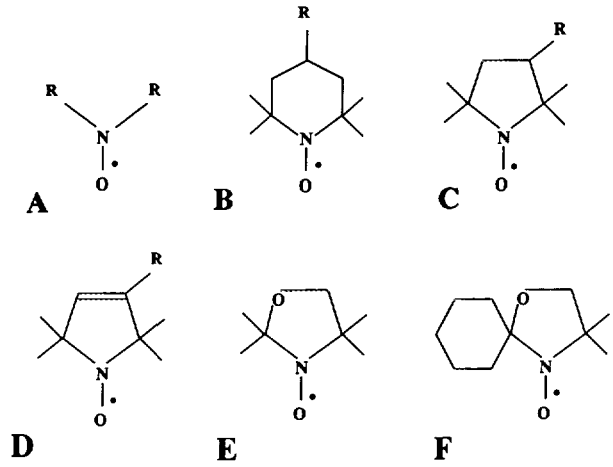

FIG. 2. Basic structures of studied nitroxides.

DTB, PCB, and SFR were purchased from Aldrich, and PCA, TOH, TNH, TPO, and TXO from Sigma. The other nitroxides used for this study were synthesized by some of the authors [i.e., AMO, DHM, and TOHD by R.C. and A.R. as described in (*11, 16*); TCA, TLA, TOL, and TPA by G.S. (*17*); and NFA by B.G. (*18*)].

The volume of the samples was 20 ml, and the nitroxide concentration was 1 m*M* in all the experiments. Sodium phosphate-buffered solutions (NaP) were made with 5 m*M* Na_2HPO_4 and 5 m*M* NaH_2PO_4 in demineralized water. Albumin solution was prepared by dissolving 42 g/liter bovine serum albumin (from Sigma) in NaP buffer. Bovine blood came from the slaughterhouse and was immediately heparinized with 15,000 IU/liter. Plasma was obtained by centrifuging blood at 2000 rpm for 15 minutes and taking the supernatant. Red-blood-cell (RBC) suspension was obtained by washing red blood cells three times with 9 g/liter NaCl. They were then diluted with the same volume of 9 g/liter NaCl solution as that of plasma removed.

N_2 and O_2 equilibration was achieved by flushing NaP solutions with N_2 and O_2, respectively, for at least 1 hour before each experiment. Gas equilibration of albumin solutions or blood samples was performed in a closed circuit composed of a rubber-sealed glass test vessel, a bubble trap, a polarographic electrode, a gas exchanger, and a roller pump (Gilson). All the components were connected with thick-wall Tygon tubing. The TrioxE0200 polarographic electrode connected to an OxI 2000 oximeter (WTW, D8120 Weilheim) was inserted in a flowthrough cell for continuous pO_2 and temperature monitoring with an accuracy of 0.1%. The gas exchanger consisted of a bundle of 20 silastic capillaries (Dow Corning) in contact with an O_2/N_2 gas mixture in a glass vessel. The dimensions of each capillary were 0.6, 1.2, and 200 mm, corresponding to inner and outer diameter and length, respectively. The equilibration of 20 ml solution with pure nitrogen to stable pO_2 = 3 mm Hg required 10 minutes.

Dynamic nuclear polarization was measured on a conventional CXP 100 Bruker spectrometer with a 13 cm gap electromagnet. In the case of SFR, the magnetic field B_0 was 6.850 mT, the EPR frequency was 199.0 MHz, and the NMR frequency was ν_H = 291.6 kHz. A frequency converter (Bru-

TABLE 1

Acronym, Chemical Name, Reference of the Basic Structure, and Side Chain of the Studied Nitroxides

Acronym	Chemical name	Basic structure	R group
AMO	2,2,5,5-tetramethyl-3-[(triethylammonium)-methyl]pyrroline-*N*-oxyl,Br^-	D	$-CH_2-N^+-(CH_2-CH_3)_3$
DHM	2,2,4,4-Tetramethyloxazolidine-*N*-oxyl	E	
DCH	3,3-Dimethyl-1-oxa-4-azospiro[4,5]dec-4-yloxyl	F	
DCP	3-Carbamoyl-2,2,5,5-Tetramethyl-3-pyrroline-*N*-oxyl	D	$-CONH_2$
DTB	Di-*t*-butyl-*N*-oxyl	A	$-C(CH_3)_3$
NFA	(2,2,5,5-Tetramethyl-1-pyrrolidinoxyl-3-carbonylamino)dodecanoate	C	$-CO-NH-(CH_2)_{11}-COOH$
PCA	2,2,5,5-Tetramethyl-3-carboxylpyrrolidine-*N*-oxyl	C	$-COOH$
PCB	3-Carbamoyl-2,2,5,5-Tetramethyl-3-pyrrolidine-*N*-oxyl	C	$-CONH_2$
SFR	Potassium nitrosodisulfonate	A	$-SO_3^-K^+$
TCA	2,2,6,6-Tetramethyl-4-carboxylpiperidine-*N*-oxyl	B	$-COOH$
TLA	Lauramido-TPO	B	$-NH-CO-(CH_2)_{10}-CH_3$
TOH	2,2,6,6-Tetramethylpiperidine-4-ol-*N*-oxyl	B	$-OH$
TOHD	Perdeutered TOH	B	$-OD$
TOL	4-Oleamido-TPO	B	$-NH-CO-(CH_2)_7-CH=CH-(CH_2)_7-CH_3$
TNH	2,2,6,6-Tetramethyl-4-aminopiperidine-*N*-oxyl	B	$-NH_2$
TPA	4-Palmitamido TPO	B	$-NH-CO-(CH_2)_{14}-CH_3$
TPO	2,2,6,6-Tetramethylpiperidine-*N*-oxyl	B	$-H$
TXO	2,2,6,6-Tetramethyl-4-oxopiperidine-*N*-oxyl	B	$=O$

Note. The basic structures are drawn in Fig. 2.

ker, Wissembourg F) changed the value ν_H of the proton resonance into a (11 MHz $- \nu_H$) signal at reception, and the (11 MHz $- \nu_H$) pulses generated by the spectrometer into pulses with a ν_H frequency at emission. These NMR pulses were amplified by a 5 W power amplifier. The measuring probe consisted of a solenoid, 10 cm long and 7 cm in diameter, tuned to the ν_H frequency and located inside a saddle coil tuned to 199 MHz for EPR. The two coils have orthogonal fields. EPR irradiation was generated by a frequency generator (Marconi Instruments, 2019a) and amplified by a 40 W power amplifier (Bruker 40 W/200 MHz). In order to take into account the second-order hyperfine interaction present at low magnetic field, the main magnetic field B_0 was always adjusted to the value which gives the maximum Overhauser enhancement factor with an EPR frequency of 199.0 MHz. This maximum corresponds to the middle EPR line of each nitroxide studied. The magnetic field was calculated by the Larmor relationship applied to the proton resonance. The NMR probe was tuned for each NMR frequency.

The pulse sequence can be divided in two periods: a polarization and an acquisition period. During the first period, lasting for 0.7 s, the middle EPR line is irradiated with the 199 MHz wave, and during the second period the free-induction decay of water protons is registered after a 90° pulse at the ν_H frequency. The repetition time was 15 seconds ($5T_{10}$) in order to always keep the equilibrium values. An irradiation period of 0.7 s was chosen on the basis of previous experiments which have shown that the measurements of the enhancement factor with four accumulations induces a temperature increase of 0.3 ± 0.05°C with a 40 W RF power source. Since the major limitation of biological applications of DNP is the overheating of the sample during EPR irradiation, we limit the EPR irradiation time to 0.7 s regardless of the relaxation time of the nitroxide solution. Therefore the enhancement factor E, with this irradiation delay, is a measure of the efficiency of DNP in biological conditions. As DNP is an exponential process with a time constant equal to the T_1 of the water protons, a 0.7 s irradiation delay with a relaxation time on the order of 1.5 seconds always gives more than a 50% saturation of the EPR line.

The water-proton polarization is calculated from the area under the recorded FID. The water-proton polarizations $\langle I \rangle$ and $\langle I \rangle_0$ were measured with and without EPR irradiation, respectively. The enhancement factor E was calculated according to Eq. [4]. E_∞, the enhancement factor at complete EPR saturation, was obtained from the reciprocal of the intercept of the regression line for an eight-point E^{-1} versus P^{-1} plot. This regression analysis also gave the slope of the regression line. The power P of the RF field used to irradiate the EPR line ranged from 40 to 12 W and was decremented by steps of 4 W.

The T_1 longitudinal relaxation time was measured with an inversion-recovery sequence and the T_2 transverse relaxation time with a Carr–Purcell–Meiboom–Gill sequence. T_1 was measured using 12 delays ranging from 10 ms to 5 s, and T_1 values were obtained with a three-parameter fit. For T_2 measurements, the interpulse delay was 20 ms and 100 echoes were recorded. The relaxativities were calculated from $R^* = (T^{-1} - T_0^{-1})/c$, where T and T_0 are the relaxation times with and without dissolved nitroxide, respectively, and c is the nitroxide concentration. All the relaxation measurements were made at low field, with 4 averages in the case of DNP and 16 averages for the pure solvent. EPR spectra were recorded at high field on an ER 200 Bruker spectrometer.

All the experiments were performed at room temperature (22 ± 2°C), and the results are expressed as the mean value $\pm$ the standard deviation of the mean. The comparisons between different experimental conditions were expressed as differences in order to benefit from statistical tests to evaluate the variations. As enhancement factors are dependent on instrumental conditions (dielectric constant of the medium and probe parameters), the enhancement factor was also normalized to PCA, which is a standard nitroxide used in many biological studies.

RESULTS AND DISCUSSION

DNP of Nitroxides in Phosphate-Buffered Solutions

Measurements of deoxygenated solutions of nitroxides are summarized in Fig. 3 and Table 2. The enhancement ranged from −36.3 for TOHD to −6.7 for TLA. The longitudinal relaxivities of the nitroxide solutions allowed them to be classified into two groups, the first with low R_1^* (below 0.7 mM^{-1} s^{-1}), and the second with high R_1^*, corresponding to nitroxides with a long side chain (NFA, TLA, TOL, and TPA). The nitroxides of the first group had R_1^* values very

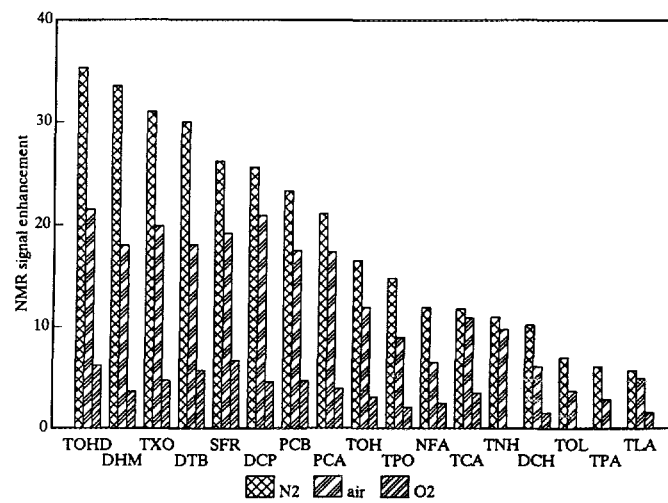

FIG. 3. Water-proton NMR signal enhancement of the studied nitroxides dissolved in NaP buffered solutions equilibrated with nitrogen, air, and oxygen. The NMR signal enhancement is the absolute value of the E factor defined by Eq. [4].

TABLE 2
DNP Parameters of the Nitroxides Dissolved in NaP Buffered Solutions

Nitroxide	B_0 (mT)	ΔW_{pp} (10^{-4} T)	E	$E\%$	R_1^* $(mMs)^{-1}$	R_2^* $(mMs)^{-1}$	Slope (a.u.)	E_∞	f	σ
AMO	6.722	1.06	−13.5	61	0.42	0.52	−0.066	−13.7	0.63	0.10
DCH	6.729	[a]	−11.2	51	0.55	0.67	−0.050	−14.9	0.69	0.10
DCP	6.715	1.74	−26.6	120	0.59	0.92	−0.018	−33.3	0.70	0.21
DHM	6.716	0.50	−34.5	156	0.40	0.52	−0.012	−41.6	0.62	0.31
DTB	6.664	0.64	−31.0	140	0.72	0.81	−0.012	−31.3	0.75	0.19
NFA	6.716	1.16	−12.9	58	0.75	0.84	−0.039	−13.4	0.75	0.07
PCA	6.705	1.12	−22.1	100	0.58	0.79	−0.017	−23.2	0.70	0.15
PCB	6.715	1.12	−24.3	110	0.57	0.76	−0.018	−31.3	0.70	0.21
SFR	6.850	0.42	−27.2	123	0.39	0.51	−0.007	−28.6	0.61	0.22
TCA	6.667	1.41	−12.8	58	0.66	0.84	−0.038	−17.5	0.73	0.11
TLA	6.668	1.68	−6.7	30	1.08	1.07	−0.181	*	0.81	−0.09
TNH	6.676	1.64	−12.0	54	0.54	0.64	−0.038	−14.3	0.68	0.10
TOH	6.669	1.51	−17.6	80	0.66	0.83	−0.039	−40.5	0.73	0.26
TOHD	6.669	0.56	−36.3	164	0.57	0.77	−0.011	−37.0	0.70	0.23
TOL	6.668	1.70	−8.0	36	1.37	1.55	−0.078	−10.4	0.85	0.06
TPA	6.668	1.70	−7.1	32	1.62	1.74	−0.057	−8.3	0.87	0.04
TPO	6.655	1.23	−15.8	71	0.50	0.74	−0.039	−18.9	0.67	0.13
TXO	6.715	0.53	−32.0	145	0.68	0.81	−0.011	−35.7	0.73	0.22

Note. B_0 is the magnetic field at which the experiment has been performed; ΔW_{pp} is the peak-to-peak EPR linewidth of samples equilibrated with air (measured at high field); E is the measured DNP enhancement factor; E% is the nitroxide enhancement to the PCA enhancement ratio in percent; R_1^* and R_2^* are the longitudinal and transverse relaxivity, respectively; slope is the slope of the E^{-1} versus P^{-1} regression line; E_∞ is the enhancement factor at complete EPR saturation; f is the leakage factor, and σ is the coupling factor.

[a] A superhyperfine structure doesn't allow the measurement of the EPR linewidth.

*E_∞^{-1} is not significantly different from 0.

close together and a mean of 0.54 ± 0.09 mM^{-1} s^{-1}. These results are in accordance with the results found in the literature (*19–22*). The discrepancy between the Overhauser enhancement and relaxivities shows that the leakage factor f, directly related to the relaxivity, is not the only factor governing the enhancement factor.

The coupling factor ranged from 0.31 for DHM to 0.04 for TPA, showing that the interaction between the nitroxide free electron and water protons was mostly of the dipole–dipole type. Only TLA, with a small negative value, showed a slight predominant scalar interaction. It can be stressed that there is a good correlation between the EPR linewidth of the nitroxides and the slope of the enhancement factor versus the RF power curve. From these results, it is clear that nitroxides with a long side chain result in poor enhancement, even though their relaxivity is far greater than that of nitroxides with small chains. A possible explanation for this could be that the acyl chain, which is hydrophobic, induces the formation of micelles when these nitroxides are dissolved in water, as the analysis of EPR spectra made by Muller *et al.* (*17*) showed.

A study of Table 2 can provide some indications for optimizing the design of new nitroxides better suited to the requirements of DNP experiments. The narrower the EPR linewidth, the greater the enhancement factor; this fact has been known for quite some time and is clearly illustrated by the increase in E between TOH and TOHD with an EPR linewidth of 1.51 and 0.56 G, respectively. As the relaxivities of all the nitroxides without a long chain residue are very close together, the second main parameter capable of modifying the enhancement factor is the coupling factor. Significantly enough, DHM has a higher coupling value than the other nitroxides. It can be postulated that the proximity of an oxygen atom from the nitrosyl group favors the coupling between the free electrons and the water protons.

Dissolved oxygen reduces the enhancement factor by acting upon the leakage factor f and the EPR linewidth. The relative decrease in enhancement factor between N_2-saturated and air-saturated solutions had a mean value of 29% and ranged from 46% for DHM to 7% for TCA. The relative decrease in leakage factor was only about 16%, while the relative slope parameter, which reflects the efficiency of the EPR saturation, had a mean value of 95%. This is evidence that in NaP solutions the sensitivity to oxygen is mainly due to the broadening of the EPR line rather than to the decrease in the f factor.

DNP of Nitroxides in Albumin Solutions

The first parameter to be taken into account when studying nitroxides dissolved in albumin solutions is the stability of the free radicals. For instance, SFR was no longer stable in albumin solutions, so no DNP enhancement could be mea-

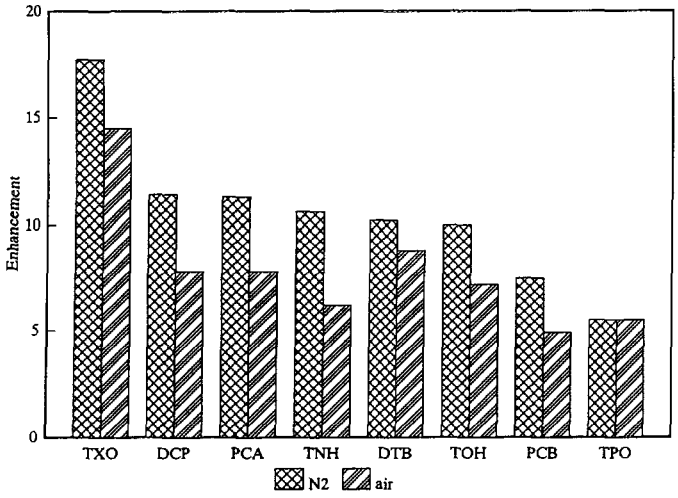

FIG. 4. Water-proton NMR signal enhancement of nitroxides dissolved in albumin solutions equilibrated with nitrogen and air.

sured. It has been shown that SFR was rapidly reduced in the presence of tyrosine and cysteine residues (*23*). The other nitroxides we studied remained stable for more than 1 day in 1 m*M* albumin solution, but DNP was less efficient than with NaP solutions. In albumin solutions, the absolute value of the enhancement factor of DNP experiments was decreased (Fig. 4). The mean difference between NaP and albumin deoxygenated solutions was 12.7 ± 4.1, corresponding to a decrease in enhancement factor of about 50%. An attempt to interpret these results using the simple model described above led to inconsistencies, such as a coupling constant greater than 0.5 for TNH and a poor correlation between the EPR linewidth and the slopes of the enhancement versus the RF regression lines. The procedure of extrapolation to complete saturation can yield erroneous values when the intersection with the ordinate is near zero, making the evaluation of E_∞ very uncertain indeed. When dealing with hydrophobic derivatives, another potential difficulty could arise from noncovalent interactions of the nitroxides with albumin (*7, 24, 25*). The EPR spectra of the albumin solution studied did not show any significant anisotropic modification of the spectra compared to those obtained with NaP solutions.

The relative influence of the various parameters on the enhancement factor will be discussed only briefly. The longitudinal relaxivities were only slightly increased, whereas their relaxivity values are far more scattered, depending on the nitroxide–albumin interaction. For example, the relaxivity of PCB varied from 0.57 $(\text{m}M\,\text{s})^{-1}$ in NaP solution to 1.35 $(\text{m}M\,\text{s})^{-1}$ in albumin solution, while that of PCA varied only from 0.58 to 0.83 $(\text{m}M\,\text{s})^{-1}$. If the relaxivity was not very much modified by the presence of albumin, it did however affect the leakage factor f, which dropped from 0.71 ± 0.02 in NaP solutions to 0.25 ± 0.19 in albumin solutions; i.e., f varied by $\Delta f/f = 65\%$. Therefore, in the presence of albumin, the loss in enhancement factor is mainly caused by the fact that proton relaxation occurs via interactions, not only with the dissolved free radicals but also with the albumin macromolecules.

The sensitivity to the oxygen content was also reduced by the presence of albumin. Nitrogen-equilibrated and air-equilibrated solutions were compared, and in the latter, the mean decrease of enhancement factor was found to be only 2.7 ± 1.3 for albumin solutions, as opposed to 20.4 ± 5.7 for the same eight nitroxides in NaP nitrogen-equilibrated solutions. The reason why oxygen in albumin solutions has such a slight effect is because its paramagnetism is insufficient to short circuit the proton relaxation mechanisms which remain short circuited by water-proton interactions. In contrast to NaP solutions, where the main relaxation process of the water protons is via the coupling with the free radicals, in albumin solutions, where the water viscosity is substantially increased, the relaxation of water is dominated by the dipole–dipole interaction between the water protons. Therefore the paramagnetism of oxygen acts only on that small part of the relaxation which is due to the electron–proton coupling.

DNP of Nitroxides Dissolved in Serum, Erythrocyte Suspension, and Whole Blood

A comparison of Figs. 4 and 5 shows clearly that the enhancement factor is lower in serum solutions than in albumin air-equilibrated solutions. The mean decrease of E was 3.9 ± 2.3, which corresponds to 46% of the enhancement obtained in albumin air-equilibrated solutions. This decrease is related to the protein concentration in serum, about 73 g/liter, while albumin concentration was only 42 g/liter. The effect of globulin is not very different from that of al-

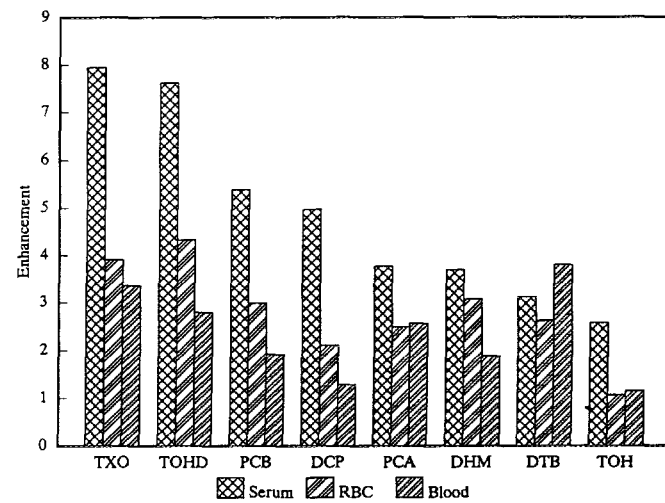

FIG. 5. Water-proton NMR signal enhancement of nitroxides dissolved in serum, red-blood-cell suspension, and whole blood equilibrated with nitrogen.

bumin. The decrease of the enhancement factor in serum can be mainly attributed to the decrease of the f factor.

In red-blood-cell suspensions, the enhancement factor of DNP was further decreased compared to the values obtained for serum, because the relaxation of water protons is increased by the presence of red blood cells, which increase the viscosity, and by the susceptibility effect of the paramagnetism of hemoglobin. The relative part of each mechanism cannot be discussed on the basis of our DNP measurements for two reasons, the first being the poor signal-to-noise ratio of these experiments, and the second being the lack of a theoretical model for such a complex system. NMR experiments performed at high magnetic fields have shown that the relaxation rates of water protons are dependent on the rate of water exchange between two frequency-shifted environments, the rate of water diffusion through local field gradients, and the interaction with paramagnetic agents such as deoxyhemoglobin (*26*). The increase in the longitudinal relaxation rate resulting from the addition of a nitroxide in this complex system is very small and consequently gives only minor DNP enhancement.

For the same reasons, the enhancement factor measured in whole blood with 1 mM nitroxide is even lower. The mean enhancement factor for the eight nitroxides studied was 2.3 ± 0.9. This value must be compared to the mean enhancement measured in NaP air-equilibrated solutions which was, for the same nitroxides, 18.2 ± 2.8. The main reason for the drop in DNP efficiency in blood compared to water solution is the decreased f factor. As a typical example, the longitudinal relaxation time of an air-equilibrated blood sample was $T_{10} = 0.17 \pm 0.01$ s and $T_1 = 0.160 \pm 0.005$ s, with the addition of PCA, giving an f factor of only 5%, which explains the poor enhancement factor of PCA dissolved in blood.

The sensitivity to oxygen of DNP in blood was also greatly reduced compared to that in NaP solutions. Figure 6 shows the enhancement factor versus the O_2 partial pressure obtained with 1 mM PCA dissolved in blood. The difference in enhancement between a blood sample equilibrated with N_2 or air was only 0.6, while in a NaP solution this difference was 3.7 for the same concentration of dissolved PCA. The reduction of the sensitivity to oxygen of DNP in blood depends on the f factor, as explained above, but the deoxygenation of hemoglobin further decreases the longitudinal relaxation time of water protons because of the paramagnetism of deoxyhemoglobin. Therefore, in red blood cells there is competition between two mechanisms: the removal of O_2 favors the relaxation of water protons by the free radicals, but it also raises the level of deoxyhemoglobin, which provides the water protons with another sink of relaxation. This limits the role of the free radicals and thus lessens the efficiency of the DNP mechanism. One way of overcoming this would be to use nitroxides which would not permeate the cell membrane, which, unfortunately, happens to be highly

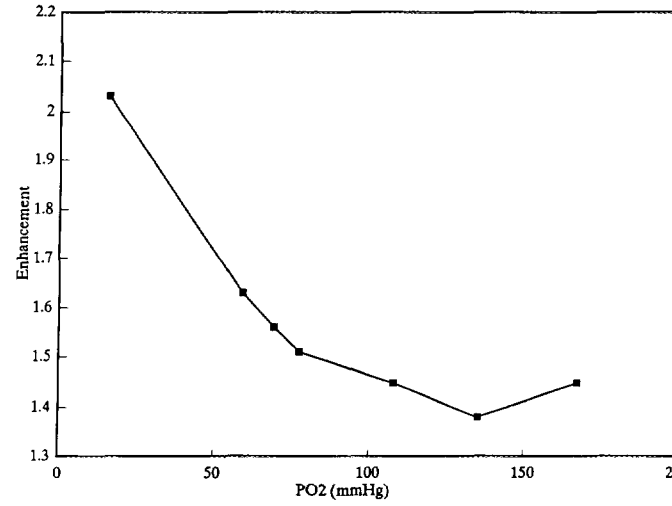

FIG. 6. Water-proton NMR signal enhancement of PCA dissolved in blood versus the oxygen partial pressure of the sample.

permeable to water molecules. In the case of rapid exchange the proton relaxation time is governed by the smallest T_1 of each of the two water compartments, and proton relaxation via the dissolved nitroxide would be in competition with relaxation via the paramagnetism of deoxyhemoglobin.

Another drawback inherent to the use of nitroxides in blood is the impaired stability of these free radicals in the presence of enzymatic and nonenzymatic reduction processes, which convert them to nonparamagnetic hydroxylamines (*27*). The poor signal-to-noise ratio of the DNP experiments with blood samples did not allow accurate measurement of the reduction rates of the nitroxides, but it was observed that five-membered ring nitroxides remained more stable than six-membered ring nitroxides. However, DHM, a nitroxide with an oxazolidine ring, was reduced fairly rapidly, even though it does have a five-membered ring structure. The presence of the oxygen atom in the ring, which favors DNP enhancement, also seems to increase the reduction rate. This observation must be related to the fact that the oxo-substituent of a nitroxide causes an unusually high reduction rate (*28*).

CONCLUSION

Until now, nitroxides have been the only free radicals to be used in biological applications of DNP. Solid radicals used in EPR oximetry, such as fusinite, synthetic carbohydrate chars, or lithium phthalocyanine derivatives, are stable in biological media and present a single EPR line with a linewidth very sensitive to oxygen pressure (*29–33*). Although it has been demonstrated that DNP in water could be induced with Li octamethoxyphthalocyanine (*34*), the small specific surface of the crystals does not allow sufficient enhancement to be useful for experiments in low magnetic

fields, even in pure water suspension. Therefore, nitroxides which are stable free radicals, highly soluble in water, and have narrow EPR lines remain the most promising free radicals for DNP experiments. Moreover, the coupling of the free electron with the nitrogen nucleus gives an EPR hyperfine structure, and, in very low fields, whereas the proton spin only experiences the applied field, the electron experiences the extra field produced by the nitrogen nuclear spin, which can be worth several times the applied field B_0. In the case of $B_0 = 0.1$ mT, the enhancement factor of DNP experiments can reach a value in excess of 2000 (*35*). In this very-low-field region, forbidden transitions become allowed and σ EPR transitions induced by an RF field parallel to B_0 become even more probable than π transitions (*36*).

Unfortunately, the use of existing nitroxides dissolved in biological fluids presents several difficulties, the first of them being a loss of stability in blood, which has been measured by EPR studies (*37*) and further demonstrated in this work. The second difficulty arises from the low relaxivity of nitroxides; e.g., at 20 MHz and 37°C, nitroxides have relaxivities of about 0.3 $(\mathrm{m}M\ \mathrm{s})^{-1}$ and when bound to serum albumin, relaxivities ranging from 1.5 to 2.5 $(\mathrm{m}M\,\mathrm{s})^{-1}$, while Gd-DTPA has a relaxivity of about 4 $(\mathrm{m}M\ \mathrm{s})^{-1}$ (*21*). As relaxivity is related to the f factor by $f = R_1^* c T_1$, a low relaxivity always induces a small f factor and therefore a poor DNP enhancement. The third difficulty concerns *in vivo* applications and derives from the potential toxicity of nitroxides. Although several works on EPR *in vivo* (*27*) described no toxicological effects of nitroxides, and although preliminary accounts would suggest that they are neither toxic nor mutagenic (*38, 39*), other works showed that some nitroxides, such as TOH, were mutagenic, particularly when in the presence of a superoxide-generating system (*40, 41*), and it has recently been shown that relatively weak doses of nitroxide lipid derivatives had levels of unexpectedly acute toxicity (*18, 42*). It seems that the nitroxide group itself is not toxic, but that the side chains can make the individual compound so. Highly lipophilic nitroxides distribute homogeneously in any cell membrane (*43, 44*), and further *in vivo* applications of nitroxides will have to take into account the fact that nitroxides are reduced by functioning cells. However, nitroxides can present potential benefits, such as a lipophilic antioxidant action (*45*) or radioprotective action (*46*).

On the basis of this work, several suggestions can be made for overcoming the difficulties encountered in the use of nitroxides in the biological applications of DNP. First, ^{15}N- and ^{2}D-substituted compounds should be used, a long-lived practice in EPR studies and DNP magnetometry (*11*). ^{15}N has a spin of $\frac{1}{2}$, which cuts the number of EPR lines down to two, and the theoretical enhancement factor of DNP can therefore reach 165 versus 110 with ^{14}N nitroxides. The small magnetogyric ratio of ^{2}D narrows the EPR line, thus facilitating the saturation of the EPR line and improving the oxygen sensitivity of DNP. Second, we suggest binding a ^{15}N, ^{2}D-substituted nitroxide either to a macromolecule or to a long side chain, with the aim of increasing the relaxivity. Binding with a macromolecule should preserve a great degree of freedom for the nitroxide, in order to avoid a broadening of the EPR lines and anisotropic modification of the EPR spectrum. When binding a nitroxide with a long side chain, one should ascertain that the chain is hydrophilic to ensure good water solubility and not to induce the formation of micelles, as happens with lipid side chains.

DNP could theoretically be of great interest in biology, especially with regards to imaging applications, because this method transfers information from free radical molecules with a high specificity and very short relaxation times to the nonspecific but very abundant water protons which have long relaxation times. Yet, progress in this field is largely conditional on the design of new nitroxides.

ACKNOWLEDGMENTS

The authors thank Dr. Pierre Antoine Bonnet for helpful discussion. Mr. Guillaume Steyaert is thanked for his help with the synthesis and DNP study of the AMO nitroxide. Special thanks are owed to Mrs. Corinne Marrer for technical assistance and Mr. Philip James for correcting the English. Active support of Bruker France is greatly acknowledged. Thierry Guiberteau benefitted from Convention CIFRE No. 357/91. This paper was partially supported by a CNRS "Interface Chimie-Biologie 1991" grant.

REFERENCES

1. D. J. Lurie, D. M. Bussel, L. H. Bell, and J. R. Mallard, *J. Magn. Reson.* **76,** 366 (1988).
2. D. Grucker, *Magn. Reson. Med.* **14,** 140 (1990).
3. D. Grucker and J. Chambron, *Phys. Med.* **5,** 329 (1989).
4. D. J. Lurie, I. Nicholson, M. A. Foster, and J. R. Mallard, *Philos. Trans. R. Soc. London Ser. A.* **333,** 453 (1990).
5. D. J. Lurie, J. McLay, I. Nicholson, and J. R. Mallard, *J. Magn. Reson.* **95,** 191 (1991).
6. H. M. Swartz, J. Bolton, and D. C. Borg, "Biological Applications of Electron Spin Resonance," Wiley, New York, 1972.
7. G. I. Likhtenshtein, "Spin Labeling Methods in Molecular Biology," Wiley, New York, 1976.
8. S. Colacicchi, M. Ferrari, and A. Sotgiu, *Int. J. Biochem.* **24,** 205 (1992).
9. A. Salvi, *Rev. Phys. Appl.* **5,** 131 (1970).
10. R. Besson, H. Lemaire, A. Rassat, A. Salvi, and P. Servoz-Gavin, XII, *in* "Electron Magnetic Resonance and Solid Dielectrics" (A. Charru and R. Servan, Eds.), p. 327, North-Holland, Amsterdam, 1964.
11. R. Chiarelli and A. Rassat, *Tetrahedron* **29,** 3639 (1973).
12. A. Abragam, "The Principles of Nuclear Magnetism," Chap. 8, Oxford Univ. Press, Oxford, 1961.
13. C. P. Slichter, "Principles of Magnetic Resonance," Chap. 7, Springer-Verlag, Berlin, 1990.
14. W. Müller-Warmuth and K. Meise-Gresch, *in* "Advances in Magnetic Resonance" (J. S. Waugh, Ed.), Vol. II, p. 1, Academic Press, New York, 1983.
15. I. Solomon, *Phys. Rev.* **99,** 559 (1955).

16. H. Caldararu, A. Caragheorgheopol, M. Dimonie, D. Donescu, I. Dragutan, and N. Marinescu, *J. Phys. Chem.* **96,** 7109 (1992).
17. P. Vallet, P. A. Bonnet, G. Subra, Y. Van Haverbeke, J. P. Chapat, and R. N. Muller, Abstracts of the Society of Magnetic Resonance in Medicine, 11th Annual Meeting, Berlin, p. 1430, 1992.
18. B. Gallez, R. Debuyst, R. Demeure, F. Dejehet, C. Grandin, B. Van Beers, H. Taper, J. Pringot, and P. Dumont, *Magn. Reson. Med.* **30,** 592 (1993).
19. K. Meise, W. Müller-Warmuth, and H. Nientiedt, *Ber. Bunsenges. Phys. Chem.* **80,** 584 (1976).
20. E. V. Goldammer, W. Kreysch, and H. Wenzel, *J. Solution Chem.* **7,** 197 (1978).
21. H. F. Bennet, R. D. Brown III, J. F. W. Keana, S. H. Koenig, and H. M. Swartz, *Magn. Reson. Med.* **14,** 40 (1990).
22. P. Vallet, Y. Van Haverbeke, P. A. Bonnet, G. Subra, J. P. Fernandez, J. P. Chapat, and R. N. Muller, Abstracts of the Society of Magnetic Resonance in Medicine, 8th Annual Meeting, Amsterdam, p. 800, 1989.
23. D. Grucker, J. Steibel, Y. Mauss, and J. Chambron, Abstracts of the Society of Magnetic Resonance in Medicine, 9th Annual Meeting, New York, p. 612, 1990.
24. M. Basset, Thesis, Université Scientifique et Médicale de Grenoble, France, 1975.
25. E. Chambaz, G. Defaye, A. Hadjian, P. Martin, R. Ramasseul, and A. Rassat, *FEBS Lett.* **19,** 55 (1971).
26. C. Casparovic and N. A. Matwiyoff, *Magn. Reson. Med.* **26,** 274 (1992).
27. A. Iannone and A. Tomasi, *Acta Pharm. Jugosl.* **41,** 277 (1991).
28. J. F. W. Keana, S. Pou, and G. M. Rosen, *Magn. Reson. Med.* **5,** 525 (1987).
29. H. M. Swartz, S. Boyer, P. Gast, J. F. Glockner, H. Hu, K. L. Liu, M. Moussavi, S. W. Norby, N. Vahidi, T. Walczak, M. Wu, and R. B. Clarkson, *Magn. Reson. Med.* **20,** 333 (1991).
30. S. W. Norby, A. I. Smirnov, S. Boyer, H. M. Swartz, and R. B. Clarkson, Abstracts of the Society of Magnetic Resonance in Medicine, 11th Annual Meeting, Berlin, p. 4107, 1992.
31. Ph. Turek, Thesis, Université Louis Pasteur, Strasbourg, France, 1989.
32. F. Bensebaa and J. J. André, *J. Phys. Chem.* **96,** 5739 (1992).
33. F. Bensebaa, P. Petit, and J. J. André, *Synth. Met.* **52,** 57 (1992).
34. T. Guiberteau, D. Grucker, J. J. André, M. Petit, and D. Lelièvre, *C.R. Acad. Sci. Ser. 2* **315,** 527 (1992).
35. A. Landesman, *J. Phys. Radium* **20,** 937 (1959).
36. T. Guiberteau and D. Grucker, *J. Magn. Reson. A* **105,** 98 (1993).
37. U. G. Eriksson, T. N. Tozer, G. Sosnovsky, J. Lukszo, and R. C. Brasch, *J. Pharm. Sci.* **75,** 334 (1986).
38. V. Azfal, R. C. Brasch, D. E. Nitecki, and S. Wolff, *Invest. Radiol.* **19,** 449 (1984).
39. D. G. Gordon, R. C. Brasch, M. D. Ogan, and D. Deen, *Invest. Radiol.* **23,** 616 (1988).
40. H. Sies and R. Mehlhorn, *Arch. Biochem. Biophys.* **251,** 393 (1986).
41. B. Gallez, C. De Meester, R. Debuyst, F. Dejehet, and P. Dumont, *Toxicol. Lett.* **63,** 35 (1992).
42. B. Gallez, R. Demeure, R. Debuyst, D. Leonard, F. Dejehet, and P. Dumont, *Magn. Reson. Imaging* **10,** 445 (1992).
43. D. O. Nettleton, P. D. I. I. Morse, W. Dobrucki, H. M. Swartz, and N. J. F. Dodd, *Biochim. Biophys. Acta* **944,** 315 (1988).
44. P. D. Morse and J. M. Yuann, *Int. J. Radiat. Appl. Instrum. A* **44,** 455 (1993).
45. Y. Miura, H. Utsumi, and A. Hamada, *Arch. Biochem. Biophys.* **300,** 148 (1993).
46. S. M. Hahn, L. Wilson, C. M. Krishna, J. Liebmann, W. De Graff, J. Gamson, A. Samuni, D. Venzon, and J. B. Mitchell, *Radiat. Res.* **132,** 87 (1992).